

The Strength Material Welding Dissimilar of Method GTAW AISI 1045 With HSS for Application Milling Tool

Toto Triantoro.B.W¹, P.Y.M Wibowo Ndaruhadi²

^{1,2}*Mechanical Engineering Dept, Universitas Jenderal Achmad Yani Bandung, Indonesia*
E-Mail: ¹trians65@yahoo.co.id; ²wibowo.ndaruhadi@lecture.unjani.ac.id

Submitted: 05-02-2023, Revised: 09-02-2023, Publication: 20-02-2023

Keywords

*Welding Dissimilar;
GTAW AISI 1045; HSS;
Mechanical Properties*

Abstract

Dissimilar welding is a permanent joining of two dissimilar materials as the application of this welding is used in milling tools that receive a large load when used. There is certainly that there is a change in the microstructure between the HAZ (Heat Affective Zone) regions, and this causes a decrease in the strength of the material, because residual stresses, defects, and cracks due to dissimilar welding will become a problem in itself. This study will connect two different materials between AISI (American Iron and Steel Institute) 1045 and HSS (High-Speed Steel), using the GTAW (Gas Tungsten Arc Welding) welding method. Welding results from tensile strength, hardness, and microstructure inspection as well as calculating grain size in the weld metal, HAZ, and base metal areas are the focus of the analysis. This dissimilar welding will compare three welding amperes that are $\pm 110A$, $\pm 167A$, and $\pm 225A$. This amperage is used based on the welding results that have been carried out for both materials with the AWS (American Welding Society) standard for circular welding of solid round materials such as the shape of a milling tool. GTAW welding method is very good and strong, but the hardness of the weld metal is large and will cause brittleness. The difference in hardness between weld metal and HAZ is significant due to the rapid heat input failing in the area between weld metal and HAZ. Tensile test results for amperage $\pm 110A$ tensile strength 84.70 kgf/mm², the hardness is 665.58 HV in the HAZ area of HSS material. Examination of the microstructure in this area has austenite, martensite, and carbide phases, it looks less than $\pm 167A$ of amperage welding, the results of the hardness test are 774.70 HV in the HAZ area of HSS material so this area will be more brittle. The smaller the grain size, the higher the hardness. The Selection of dissimilar welding filler metal produces good joint strength. While the amperage welding of $\pm 225A$ broke on welded metal with a tensile strength of 43.41 kgf/mm², the hardness in the HAZ area was made of HSS with a hardness of 772.37 HV. The smallest hardness value is in the base metal area of AISI 1045 material with a hardness of 264.45 HV. The difference in hardness is much different between HSS and AISI 1045, indicating the use of filler metal with poor connection strength for large amperes.

1. Introduction

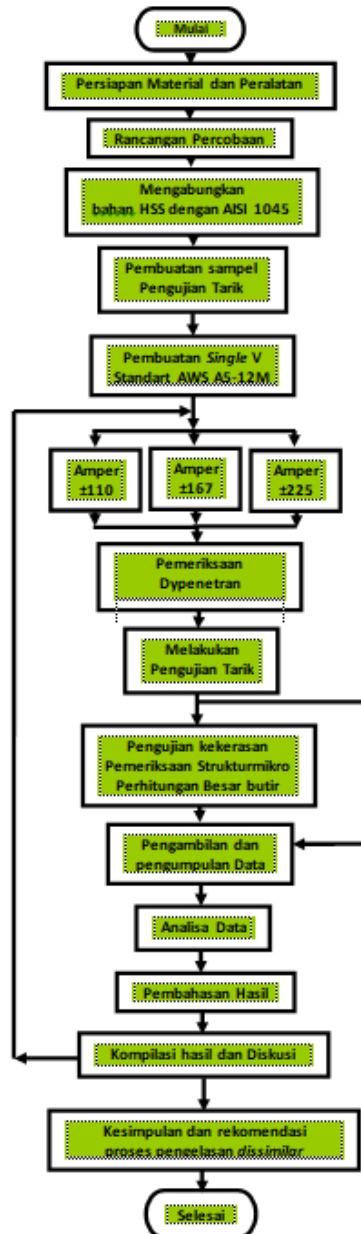
The development of welding technology to obtain the strength of welding joints. In dissimilar welding as a milling tool splicing application. Welding with low cost is needed in the world of the medium manufacturing industry. The sluggish manufacturing industry due to the outbreak of the COVID-19 virus has prompted researchers to conduct studies, especially regarding dissimilar welding technology. Welding is part of the manufacturing industry in developing countries such as Indonesia; this will increase the income of the middle to lower industrial sector (Groover, 2006). Strong construction makes welding one of the choices in industrial engineering construction. The quality of the welding results can not only be seen visually but must be known in a structured manner with various forms of application [10] (Perdana et al., 2019).

The most popular welding uses an electric arc, including the GTAW method. This welding is for lightweight construction, so it can withstand high strength, is easy to implement, and is quite economical. The main weakness is the occurrence of changes in the microstructure of the welded material, especially for dissimilar welding, so that it is possible to change the physical and mechanical properties of the welded material (Wardoyo et al., 2014). Determining the welding parameters in the dissimilar welding process is a separate obstacle in this study. In addition to these weaknesses, the results of dissimilar welding, among others, will occur a large voltage spike from one of the materials which is an obstacle when determining the welding amperage that is not precise. Inappropriate selection of parameters will cause changes in the microstructure including the welding area and the HAZ area so that there will be a decrease in the strength of the material in that area, residual stresses, and defects will appear, cracks will occur due to the welding (Weman, 2011).

Based on the background above, this research can formulate several problems that will be raised as the formulation of the problem:

1. To obtain dissimilar welding amperage, as the strength of the connection resulting from the GTAW method of welding on two different materials for application in milling tools.
2. Analyzing the results of dissimilar welding between AISI 1045 material and HSS material, in circular welding of solid round materials as milling tool applications including: tensile strength, hardness and microstructure inspection as well as calculating grain size in the weld metal, HAZ and base metal areas.

To get the optimal welding amperage based on the AWS A5-12M welding standard in dissimilar welding, joining different materials with the GTAW welding method, as an application for tool milling in further research (Arc, n.d.). Obtaining dissimilar welding amperage with the GTAW method based on the AWS standard between AISI 1045 steel and HSS material by varying the welding ampere, namely, $\pm 110A$, $\pm 167A$, and $\pm 225A$, this welding amperage data is the best ampere from previous research (Wiryo Sumarto & Okumura, 2000). It is expected to be a reference and input for the dissimilar welding process with AWS standards with low and economical operational costs in terms of operations and processes for middle and lower manufacturing industry players related to the welding process, solid round shape, application to tool milling equipment or other applications (Black & Kohser, 2017).

Figure 1. Research flow chart

2. Research Method

The research method was carried out, with experimental and absorption methods, materials, and equipment were prepared. Then it is analyzed as shown in Figure 1, the planned research flow diagram to facilitate the stages of the research process.

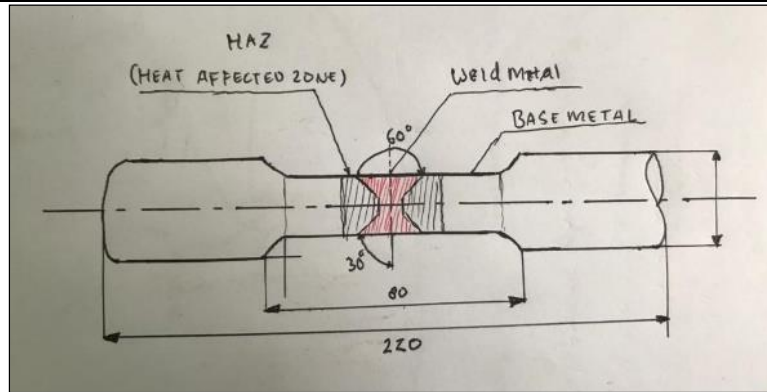


Figure 2. Design sample tensile test

Tensile testing is a mechanical test that aims to determine the strength of a metal, including; tensile strength, yield strength, and strain. Before welding, the workpiece is turned and made a seam angle, using a lathe according to the ASTM (American Test and Material Association) A-370 tensile testing standard size, with a single V seam shape on each test sample as shown in Figure 2 above (Zukauskaite et al., 2013).

3. Results and Discussions

The first step is the process of making tensile samples referring to the ASTM E-370 standard, using a universal lathe on both types of materials, namely, AISI 1045 material and HSS material. Followed by the process of making a welding seam, namely a single V seam with an angle of 60°



Figure 3. Tensile test sample production.

Welding Process.

In the GTAW method welding process for AISI 1045 medium carbon steel and HSS with a workpiece diameter of 20 mm and a length of 220 mm, all amperes are varied in two stages, the first stage is rooting, the second stage is filler



Figure 4. Welding dissimilar method GTAW at each welding ampere condition.

Table 1: Result welding GTAW with ampere $\pm 110A$

No	Process type	Filler Metal		Amper/Voltage		Polarity
		Type	Diameter (mm)	Ampere (A)	Volt (V)	
1.1	GTAW	ER 90S	2,4	± 110	24	DCEN
1.2	GTAW	ER 90S	2,4	± 110	24	DCEN
1.3	GTAW	ER 90S	2,4	± 110	24	DCEN



Figure 5 Result welding dissimilar ampere $\pm 110A$

Table 2: Result welding GTAW with ampere $\pm 167A$

No	Process type	Filler Metal		Amper/Voltage		Polarity
		Type	Diameter (mm)	Ampere (A)	Volt (V)	
1.1	GTAW	ER 90S	2,4	± 167	24	DCEN
1.2	GTAW	ER 90S	2,4	± 167	24	DCEN
1.3	GTAW	ER 90S	2,4	± 167	24	DCEN



Figure 6. Result welding dissimilar ampere $\pm 167A$

Table 3: Result welding GTAW with ampere $\pm 225A$

No	Process type	Filler Metal		Amper/Voltage		Polarity
		Type	Diameter (mm)	Ampere (A)	Volt (V)	
1.1	GTAW	ER 90S	2,4	±225	24	DCEN
1.2	GTAW	ER 90S	2,4	±225	24	DCEN
1.3	GTAW	ER 90S	2,4	±225	24	DCEN



Figure 7. Result welding *dissimilar* ampere ±225A

The next stage after the welding process is complete is to clean the capping contained in the results of the welding process. The cleaning of the welding capping is carried out utilizing a lathe process using a carbide lathe. Figure 8 below is a picture of the capping cleaning process that occurs from the results after the dissimilar welding process.



Figure 8. Result process remove capping

Heat Input Calculation.

The welding heat input comes from the electric arc using the following equation:

$$HI = \frac{I \times V \times 60}{TS} \text{ kj/mm}$$

Dimana :

I : Arus
V : Voltase
TS : Travel Speed

Welding specimens with an ampere of ±110A of welding heat input were obtained at 487.38 Kj/mm. While the amperage welding specimen is ±167A, the welding heat input is 498.92 Kj/mm. Welding specimens with amperage of ±225 welding heat input of 682.10 Kj/mm. So the greater the welding amperage, the greater the heat input.

Non- Destructive Inspection.

Using the dy-penetrant (NDT) method it will provide visual information on the occurrence of cracks. This can be obtained by using a tool in the form of a liquid that has a specific color, including: red or a color that will move under ultra violet light. Of course the cracks are thin enough that they can't be seen with the naked eye. After all the samples were cleaned using MD125 thinner, the dy-penetrant was sprayed. The next step, the sample is cleaned again with MD125 thinner liquid followed by spraying developer liquid.



Figure 9. Result process liquid spray dy-penetrant.

Thus, the liquid part of the developer will coat the area above the crack and change color. If the liquid penetrant used is red, the defects or cracks will appear and turn red.



Figure 10. Result process liquid spray developer

The results of the dy-penetrant inspection for ± 110 Ampere amperage showed that one sample was cracked. As for the amperage of ± 167 amperes, the dy-penetrant fluid appeared in all the crack samples clearly visible. For an amperage of ± 225 Amper, one sample looks cracked.

Tensile Test.

Tensile testing is carried out using the ASTM A-370 standard. By using the Instron brand tensile testing machine with a maximum capacity of 20 tons, with an engine movement rate of 1.3 – 2.5 mm/minute at a test temperature of around 26°C. Sample testing was carried out with three samples each with varying conditions of welding amperage in this study.

Table 4: Result tensile strength variation ampere

No	Sample	Ultimate Tensile Strength (Mpa)	Tensile Stress Yield (Offset 2%) (Kgf/mm ²)	Maximum Load (KN)	Description
Arus ±110 Amper					
1	Sample S.1.1	83,94	52,64	11,927	Break in <i>weld metal</i>
2	Sample S.1.2	84,13	53,80	10,962	Break in <i>base metal</i>
3	Sample S.1.3	86,16	54,93	12,149	Break in <i>base metal</i>
	Average	84,74	80,19	11,679	
Arus ±167 Amper					
1	Sample S.2.1	53,20	39,54	7,413	Break in <i>weld metal</i>
2	Sample S.2.2	30,31	17,13	4,004	Break in <i>weld metal</i>
3	Sample S.2.3	37,01	25,08	5,126	Break in <i>weld metal</i>
	Average	40,17	27,25	5,543	
Arus ±225 Amper					
1	Sample S.3.1	89,07	55,90	11,245	Break in <i>weld metal</i>
2	Sample S.3.2	96,06	69,48	13,146	Break in <i>base metal</i>
3	Sample S.3.3	43,41	26,66	06,086	Break in <i>base metal</i>
	Average	76,38	50,68	10,159	

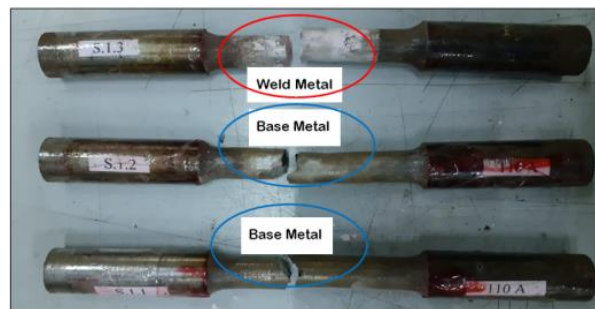


Figure 11. Result tensile strength for ampere ±110A

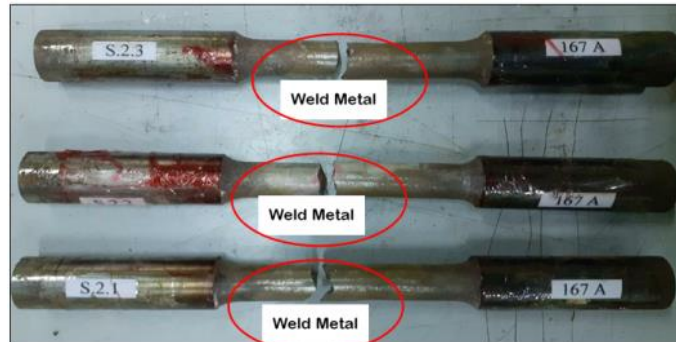


Figure 12. Result tensile strength for ampere ±167A

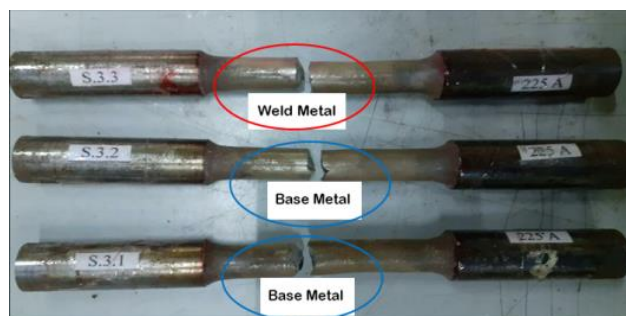


Figure 13. Result tensile strength for ampere ±225A

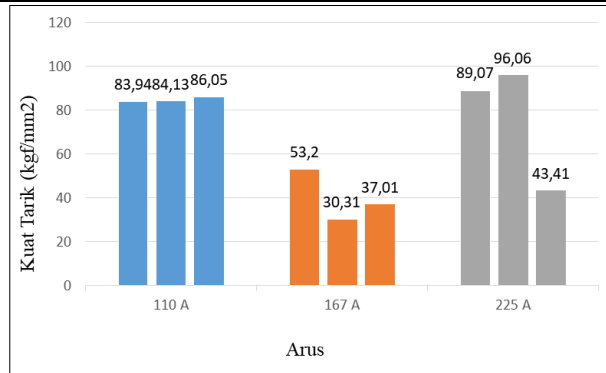


Figure 14. Graph of tensile strength every ampere

Based on the test results, as in table 4 above for amperes ±110A the tensile strength is 83.94 kgf/mm² and 84.13 kgf/mm². This indicates that the welding connection with filler metal used and the welding parameters carried out, one of which is welding amperage, results in good joint strength. For welding amperage ±167A the tensile strength is 53.20 kgf/mm² and 37.01 kgf/mm² where the welding heat input affects the mechanical properties of the material itself. For welding amperage ±225A with a tensile strength value of 89.07 kgf/mm² while for S.3 3 specimens, it breaks in the weld metal area with a tensile strength value of 43.41 kgf/mm²

Hardness Test.

Hardness testing was carried out using the Vickers method with the ASTM E-92 standard. Data collection was carried out after tensile testing, hardness testing was carried out at 15 points, namely; three points in the base metal of AISI 1045 material, three points in the base metal region of HSS material, three points in the heat-affected area of AISI 1045 and, HSS materials, and three points in the weld metal area.

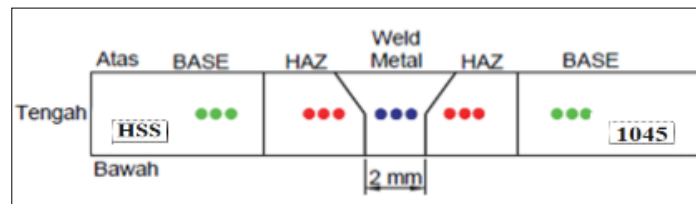


Figure 15. Hardness testing area position.

Hardness testing was carried out using an Alfa durometer machine with the Vickers method with a load of 300 grams, the type using a diamond pyramid indenter with a pyramid angle of ±136°.

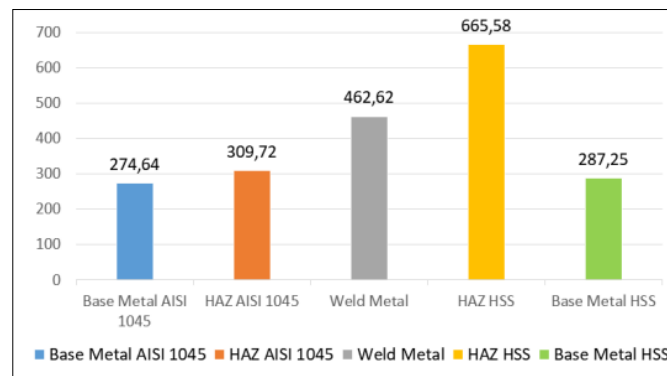


Figure 16. Average hardness value on ampere ±110A.

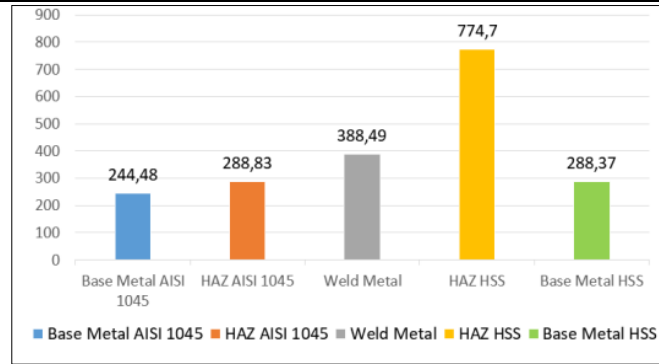


Figure 17. Average hardness value on ampere $\pm 167A$.

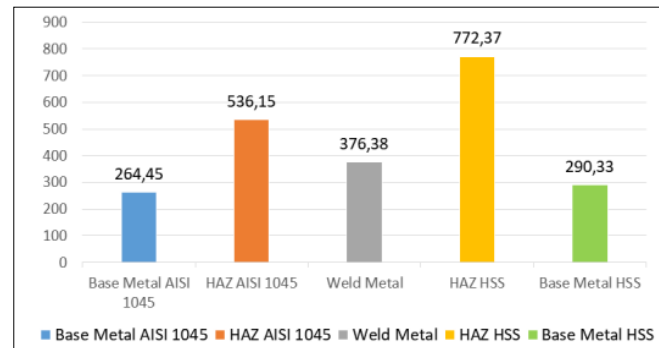


Figure 18. Average hardness value on ampere $\pm 225A$.

From the data, the highest average hardness value is in the weld metal area at welding amperage $\pm 110A$ with a hardness value of around 462.62 HV, while in the HAZ area, the hardness value is around 665.58 HV, and in the base metal area of AISI 1045 the hardness value is around 274.64 HV, and base metal HSS hardness value of about 309.72 HV. While the average hardness value for welding amperage $\pm 167A$ weld metal area 388.49 HV, HAZ area HSS material 774.7 HV, and HAZ area AISI material 1045 around 288.83 HV.

While the average hardness value for welding amperage $\pm 225A$, the weld metal region is 376.38 HV, The HAZ region HSS material is 772.37 HV, and the HAZ area is AISI material 1045 536.48 HV. Meanwhile, for welding amperage $\pm 110A$, the value of hardness in the weld metal area is 462.62 HV and the hardness value in the HAZ area of HSS material is 665.58 HV and the hardness value is in the HAZ area of AISI 1045 309.64 HV material. Where the difference in hardness values between the weld metal area and the two materials in the HAZ area is quite small compared to the welding amperage of $\pm 167A$ and $\pm 225A$.

Microstructure Inspection.

Examination of the microstructure to determine the structure formed in the three areas of dissimilar welding between AISI 1045 material and HSS material, namely, weld metal, HAZ and base metal areas (Ritonga & Purwaningsih, 2018). The preparation stage for microstructure inspection is done by cutting each sample using a disc-cutting machine, then a grinding process is carried out with an increase in sandpaper roughness from 300 to 4000. Followed by the polishing process using bludru cloth and using paste. Using a certain optical microscope that has the ability to magnify up to 500x, the microstructure can be examined after loading, namely after tensile testing.

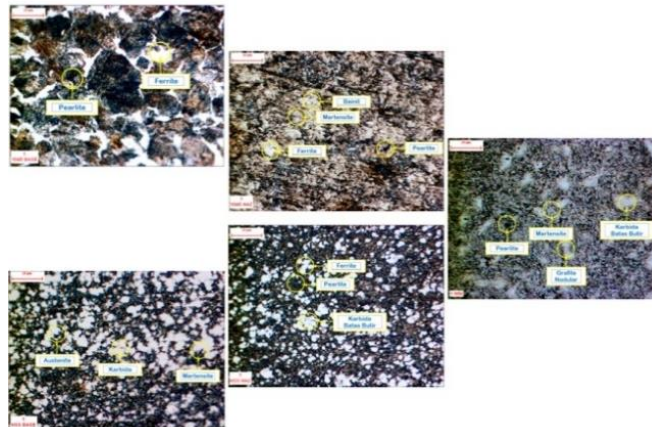


Figure 19. Microstructure of ampere ampere±110 welding result in three weld areas materials AISI 1045 & HSS

In the base metal area of AISI 1045 ampere welding $\pm 110A$ 500x magnification, the white ferrite phase fused in pearlite looks dark in the large fused area, in the balance between ferrite and pearlite. In the base metal area of HSS material, there is an austenite phase, which is a solid solution of free carbon and iron in gamma iron. A small amount of carbide and martensitic in the HAZ AISI 1045 area is affected by heat with a sharp shape and a little bainite with a fine sharp shape, is also in the HAZ area of the HSS material. In the weld metal area, the ferrite phase changes to a nodular graphite phase and a little iron carbide so that in this area it is slightly harder than in the two base metal regions.

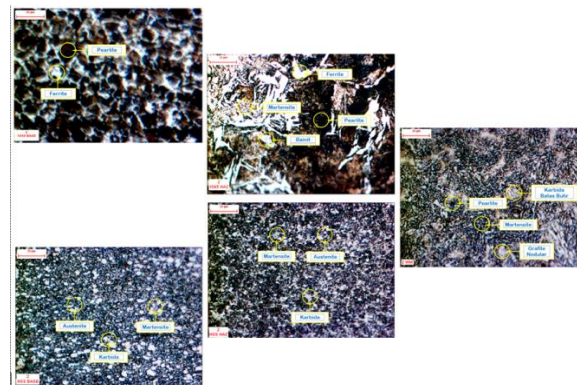


Figure 20. Microstructure of ampere ampere±167 welding result in three weld areas materials AISI 1045 & HSS.

While the welding amperage is $\pm 167A$ in the base metal area of AISI 1045 material, the pearlite phase is more visible than the ferrite phase which is getting smaller and smaller. Likewise, in the base metal area, the austenite, martensite and iron carbide phases of HSS materials are more visible than the amperage of $\pm 110A$. The grain shape also decreases uniformly indicating an increase in hardness.

While the welding amperage of $\pm 167A$ AISI 1045 material for the HAZ region, the pearlite and ferrite phases re-assembled were larger but the pearlite phase was more abundant than the ferrite. While the martensite and bainite phases with higher welding amperage will be more numerous. The bainite phase is formed from ferrite and cementite which is sharp long soft or in the form of plates arranged depending on the welding amperage.

For the weld metal pearlite area is seen very little and the ferrite phase is absent, martensitic is seen a lot. The nodular graphite and carbide phases increase with increasing welding amperage and hardness increases.

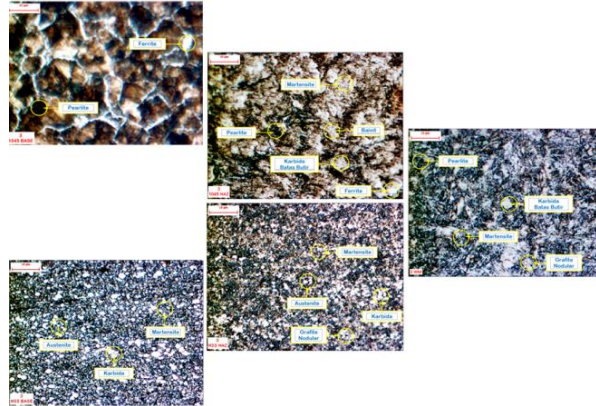


Figure 21.Microstructure of ampere amper ±225 welding result in three weld areas materials AISI 1045 & HSS.

At the welding amperage of ±225A, the AISI 1045 material still has ferrite and pearlite turns into cementite. Meanwhile, in the HSS base metal area, there is a small amount of austenite, martensite, and carbide.

The austenite phase is a solid solution of free carbon (ferrite), and iron (Fe) in gamma. Heating the steel, after the upper critical temperature, the formation of the finished structure becomes a hard, ductile, and non-magnetic austenite. This condition is able to dissolve large amounts of carbon, and transfer occurs during the heating and cooling of the workpiece (Rudiyanto et al., 2022). In the HAZ area, the AISI 1045 ferrite and pearlite, and martensite materials are much reduced in the form of a smaller structure but, more and more bainite is seen. This phase is formed from ferrite and cementite is formed with higher amperage, whereas bainite will increase with increasing temperature.

In the weld metal region, the pearlite and ferrite phases are almost absent. Martensite is almost evenly distributed, as are the nodular graphite and carbide phases. This is evidenced by the high value of violence in this area.

Grain Size Calculation.

The formula for calculating grain size using the Heyne method is:

$$D_m = \frac{L \cdot p \cdot 10^3}{Z \cdot V} (\mu m)$$

Diketahui: L : Panjang garis 60 mm
 p : Jumlah garis 6
 Z : Jumlah butir terpotong
 V : Pembesaran struktur mikro

Table 5: Calculation of grain size in each condition

NO	Sample	Zone	Value Z	Large value of grains
1	±110 A AISI 1045	Base metal	2400	145 μm
2		HAZ	2500	136 μm
3		Weld metal	3100	127 μm
1	±167 A AISI 1045	Base metal	2420	146 μm
2		HAZ	2520	139 μm
3		Weld metal	2560	128 μm
1	±225 A AISI 1045	Base metal	2394	149 μm
2		HAZ	2553	131 μm
3		Weld metal	2610	142 μm
1	±110 A HSS	HAZ	3500	115 μm
2		Base metal	2510	149 μm
1	±167 A HSS	HAZ	3511	103 μm
2		Base metal	2521	138 μm
1	±225 A HSS	HAZ	3507	110 μm
2		Base metal	2527	136 μm

4. Conclusion

The highest average tensile strength value of the specimen with amperage $\pm 110A$ is 84.70 kgf/mm², while the lowest tensile strength is at amperage $\pm 167A$ at 40.17 kgf/mm². From the results of the ampere hardness test $\pm 110A$, the highest hardness value of 665.58 HV is found in the HAZ area of the HSS material. For amperes $\pm 167A$ the highest hardness value is 774.70 HV which is found in the HAZ area of the HSS material. For amperes $\pm 225A$ the highest hardness value is 772.37 HV in the HAZ area of HSS material. For this reason, the HSS material in the HAZ area with the highest hardness value can be said to be very strong and brittle.

The results of the microstructure examination, obtained the Heat Affected Zone area of HSS material with 500x magnification, visible phases of austenite, cementite, martensite and bainite and carbide indicating that this area has the highest hardness. Likewise in the weld metal area, these phases are dominantly visible. The grain size calculation is, as a control for the hardness test, the smaller the grain size, the harder the area.

5. References

- Arc, G. T. (n.d.). *Guidelines For Gas Tungsten Arc Welding (GTAW)*.
- Black, J. T., & Kohser, R. A. (2017). *DeGarmo's materials and processes in manufacturing*. John Wiley & Sons.
- Groover, M. P. (2006). *Fundamentals of modern manufacturing, 2002*. Bethlehem: John Wiley & Sons.
- Perdana, S., Budiarto, U., & Santosa, A. W. B. (2019). Pengaruh Variasi Waktu Penahanan (Holding Time) pada Perlakuan Panas Normalizing Setelah Pengelasan Submerged Arc Welding (SAW) pada Baja SS400 terhadap Kekuatan Tarik, Tekuk dan Mikrografi. *Jurnal Teknik Perkapalan*, 8(1), 21–30.
- Ritonga, A. S., & Purwaningsih, E. S. (2018). Penerapan Metode Support Vector Machine (SVM) Dalam Klasifikasi Kualitas Pengelasan Smaw (Shield Metal Arc Welding). *Jurnal Ilmiah Edutic: Pendidikan Dan Informatika*, 5(1), 17–25.
- Rudiyanto, A., Anjani, R. D., & Naubnome, V. (2022). Analisis Proses Stress Relieving Annealing Terhadap Sambungan Las Gas Metal Arc Welding (Gmaw) Material Baja SS 400. *Jurnal Ilmiah Wahana Pendidikan*, 8(22), 84–93.
- Wardoyo, T. T. B., Izman, S., & Kurniawan, D. (2014). Effect of Butt Joint on Mechanical Properties of Welded Low Carbon Steel. *Advanced Materials Research*, 845, 775–778.
- Weman, K. (2011). *Welding processes handbook*. Elsevier.
- Wiryosumarto, H., & Okumura, T. (2000). Teknologi pengelasan logam, PT. *Pradnya Paramita, Jakarta*.
- Zukauskaitė, A., Mickevičienė, R., Karnauskaitė, D., & Turkinė, L. (2013). Environmental and human health issue of welding in the shipyard. *Transport Means 17th International Conference, 2013*.
<https://www.pengelasan.net/wp-content/uploads/2016/12/Welding-Torch.jpg> diakses (12/10 2020)
<https://www.pengelasan.net/wp-content/uploads/2016/12/Jenis-tipe-Tungsten-GTAW.png> diakses (12/10 2020)
Dionisius Younggi.cuttingtool,material.2019.Diaksesdarihttp://Teknik mesin manufaktur. Diakses (20 februari 2020)



© 2023 by the authors. Submitted for possible open access publication under the terms and conditions of the Creative Commons Attribution (CC BY SA) license (<https://creativecommons.org/licenses/by-sa/4.0/>).